

RESEARCH

Open Access



ZNF169 promotes thyroid cancer progression via upregulating FBXW10

Wen Luo¹, Qiyu Xiao¹ and Ying Fu^{1*}

Abstract

Background Zinc finger protein 169 (ZNF169) plays a key role in cancer development. However, the specific role of ZNF169 in the tumorigenesis of thyroid carcinoma (THCA) remains poorly understood.

Methods The expression of ZNF169 was measured using immunohistochemistry, RT-qPCR, and western blot. Cell proliferation was detected using CCK-8 assay and cell colony formation assays, while cell migration was determined by Transwell assay. Flow cytometry was used to detect cell apoptosis and cell cycle distribution. The interaction of ZNF169 and its downstream gene was studied using luciferase assay and CHIP-PCR. Recovery assay in cells and animals were also performed to demonstrate the mechanism.

Results ZNF169 was highly expressed in THCA tissues and cells lines compared with matched adjacent non-cancerous thyroid tissues or normal thyroid epithelial cell. Moreover, thyroid cancer cell proliferation and migration were suppressed following ZNF169 knockdown, while were potentiated by ZNF169 overexpression. ZNF169 also regulate THCA cell apoptosis and cell cycle progression. Mechanically, ZNF169 enhanced the transcription activity and expression of F-box/WD repeat-containing protein 10 (FBXW10) via the binding to its promoter. There was a positive correlation between ZNF169 and FBXW10 in THCA patients. In addition, knockdown of FBXW10 suppressed the proliferation of THCA cells. Recovery assays in vitro and in vivo demonstrated that FBXW10 knockdown reversed the effects of ZNF169 overexpression on THCA cell proliferation and tumor growth.

Conclusions In summary, ZNF169 promotes THCA progression via upregulation of FBXW10, which may provide a novel theoretical basis for the development of clinical therapies for THCA.

Keywords Zinc finger protein 169, Thyroid cancer, F-box/WD repeat-containing protein 10, Cell proliferation

Background

Thyroid cancer originates from cells of the thyroid gland, and is the most common endocrine malignancy [1–3]. The incidence rates of THCA have steadily increased over the past few decades [1]. In the United States, the incidence of thyroid cancer increased by 211% between 1975 and 2013 [4]. The majority of thyroid cancers (>95%), which are derived from follicular cells, are indolent tumors that can be effectively cured with a combination of surgical resection and radioactive iodine ablation [5, 6]. The 5-year survival rates of well-differentiated thyroid carcinoma are ~93% for women and ~88% for men

*Correspondence:

Ying Fu
fuyin@hnca.org.cn

¹Department of Nuclear Medicine, The Affiliated Cancer Hospital of Xiangya School of Medicine, Central South University/Hunan Cancer Hospital, No. 283 Tongzipo Road, Yuelu District, Changsha 410013, Hunan, P.R. China



© The Author(s) 2024. **Open Access** This article is licensed under a Creative Commons Attribution-NonCommercial-NoDerivatives 4.0 International License, which permits any non-commercial use, sharing, distribution and reproduction in any medium or format, as long as you give appropriate credit to the original author(s) and the source, provide a link to the Creative Commons licence, and indicate if you modified the licensed material. You do not have permission under this licence to share adapted material derived from this article or parts of it. The images or other third party material in this article are included in the article's Creative Commons licence, unless indicated otherwise in a credit line to the material. If material is not included in the article's Creative Commons licence and your intended use is not permitted by statutory regulation or exceeds the permitted use, you will need to obtain permission directly from the copyright holder. To view a copy of this licence, visit <http://creativecommons.org/licenses/by-nc-nd/4.0/>.

[7]. However, a subset of the patients are diagnosed at aggressive stage. Some of the patients at advanced stage can be benefitted from targeted therapies or immunotherapies, whereas numbers of the patients still face the situations with no effective therapeutic options currently available [8–10]. Thus, further investigations into novel therapeutic strategies are required for the effective treatment of thyroid cancer.

Various types of thyroid cancers include thyroid carcinoma (THCA), follicular thyroid carcinoma (FTC), Hürthle cell carcinoma, medullary thyroid carcinoma (MTC) and anaplastic thyroid carcinoma (ATC) [2, 11]. Within each type, a number of mutations lead to increased cellular proliferation and dedifferentiation [12]. Papillary thyroid carcinoma (PTC) is the most common type of human THCA [13]. Within PTC, B-Raf proto-oncogene, serine/threonine kinase (BRAF) point mutations and proto-oncogene tyrosine-protein kinase receptor Ret /PTC rearrangements are the most prominent genetic alterations, which account for 40–60% and 20% of cases, respectively. These mutations may have the potential to act as targets for the treatment and diagnosis of the most aggressive forms of PTC [14, 15]. Within FTC, KRAS proto-oncogene, GTPase (KRAS) point mutations account for 45% of cases, and paired box 8 (PAX-8)/ peroxisome proliferator activated receptor gamma (PPAR γ) rearrangements account for 35% of the cases. During the mutation of KRAS proteins, the mitogenic mitogen-activated protein kinase (MAPK) and phosphatidylinositol-4,5-bisphosphate 3-kinase (PI3K) pathways are activated, which may serve as potential therapeutic targets [16]. Further mutations in the tumor suppressor gene phosphatase and tensin homolog (PTEN) account for 10% of cases, and mutations in the PI3KCA oncogenes account for 10% of cases within this tumor type [17, 18]. Genetic alterations that lead to the development of ATC may also be found in PTC and FTC, and mutations in the tumor protein p53 (TP53) and β -catenin genes are also observed [19, 20].

Zinc finger protein 169 (ZNF169) is a nuclear protein that contains one Krüppel-associated box (KRAB) domain and 13 Cys2-His2 (C2H2)-type zinc fingers. ZNF169 is widely expressed in the kidneys, spleen, liver, small intestine, and heart, where it functions as a transcription regulator. The gene encoding ZNF169 maps to a region of human chromosome 9q22, which has been associated with numerous diseases, such as colon cancer, migraine auras, basal cell carcinoma, Gorlin syndrome and extra skeletal myxoid chondrosarcoma. Previous studies into the specific function of ZNF169 are limited, and the results of a recent study indicated that ZNF169 is a human obesity gene [21]. Moreover, results from a previous study also demonstrated that ZNF169 may be

associated with self-healing squamous epitheliomata (ESS1) [22].

F-box/WD repeat-containing protein 10 (FBXW10) is located on chromosome 17p12 and is a member of the FBXW family of protein ubiquitin ligases [23–26]. Methylation of FBXW10 is increased in cancer tissues, which is significant for tumor invasion [23]. FBXW10 is also highly expressed in hepatocellular carcinoma (HCC) tissues in male patients, and is associated with HCC tumorigenesis and the probability of survival [24].

To the best of our knowledge, the present study was the first to investigate the involvement of ZNF169 in THCA progression. The effects of ZNF169 knockdown and overexpression on tumor cell proliferation and invasion were investigated, and whether these effects were mediated by FBXW10 was also examined. We found that overexpression of ZNF169 contributed to the development of THCA through upregulating FBXW10, which may lead to the development of novel diagnostic and therapeutic options for thyroid cancer.

Results

ZNF169 is overexpressed in human THCA

To investigate the role of ZNF169 in THCA progression, ZNF169 expression in THCA tissues was evaluated using immunohistochemical analysis. ZNF169 was highly expressed in THCA tissues compared with matched adjacent healthy tissues (Fig. 1A; Table 1). RT-qPCR and western blot results also showed that the expression of ZNF169 was highly expressed in three THCA cells as compared to normal human primary thyroid follicular epithelial cell Nthy-ori 3–1 (Fig. 1B, C). These data showed the high expression of ZNF169 in THCA.

ZNF169 knockdown suppresses cell proliferation and migration

To explore the role of ZNF169 in THCA progression, shRNAs was used to infect TPC1 and BCPAP cells. Western blot and RT-qPCR results confirmed the knockdown efficiency following transfection with shZNF169s in TPC1 and BCPAP cells (Fig. 2A and B). CCK-8 results demonstrated that ZNF169 knockdown markedly suppressed the proliferation of TPC1 and BCPAP cells (Fig. 2C). Moreover, the results of the colony formation assays demonstrated that fewer colonies were formed by shZNF169 cells compared with the shCtrl group (Fig. 2D). In addition, following ZNF169 knockdown, the cell migration ability was impaired, as the percentage of migrated cells was markedly decreased in TPC1 and BCPAP cells compared with the control cells (Fig. 2E). We also found that ZNF169 knockdown resulted in upregulation of p21 and E-cadherin, and downregulation of N-cadherin and Vimentin (Figure S1). Collectively,

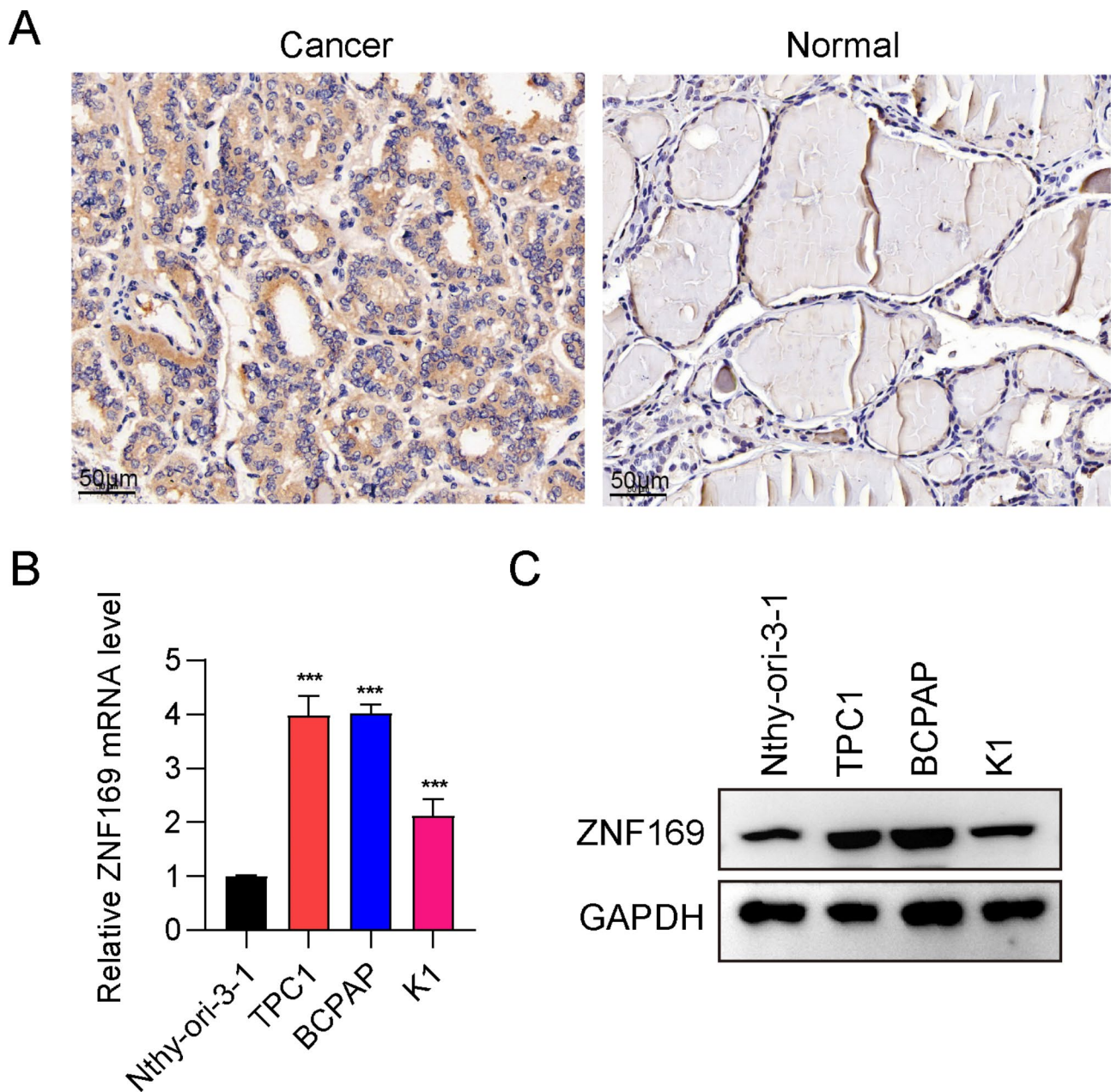


Fig. 1 ZNF169 is overexpressed in THCA tissues. **(A)** ZNF169 expression was evaluated using immunohistochemical staining of THCA tissues and matched adjacent healthy thyroid tissues. **(B)** ZNF169 mRNA expression in three THCA cell lines (TPC1, BCPAP, K1) and a normal human primary thyroid follicular epithelial cell (Nthy-ori 3 – 1) were measured using RT-qPCR. **(C)** ZNF169 protein expression in three THCA cell lines (TPC1, BCPAP, K1) and a normal human primary thyroid follicular epithelial cell (Nthy-ori 3 – 1) were measured using western blot. Magnification, $\times 200$

Table 1 The expression of ZNF169 in PTC and normal tissues

Type	ZNF169 expression		χ^2	P-value
	Low	High		
Normal tissues	23	2	32.05	< 0.001
PTC	3	22		

these results highlighted the role of ZNF169 as an oncogene.

ZNF169 overexpression promotes cell proliferation and migration

As ZNF169 has the potential to act as an oncogene, it was hypothesized that ZNF169 overexpression may promote tumor progression. RT-qPCR and Western blot analyses were performed to verify the overexpression of ZNF169 in both K1 cells (Fig. 3A and B). Cell viability

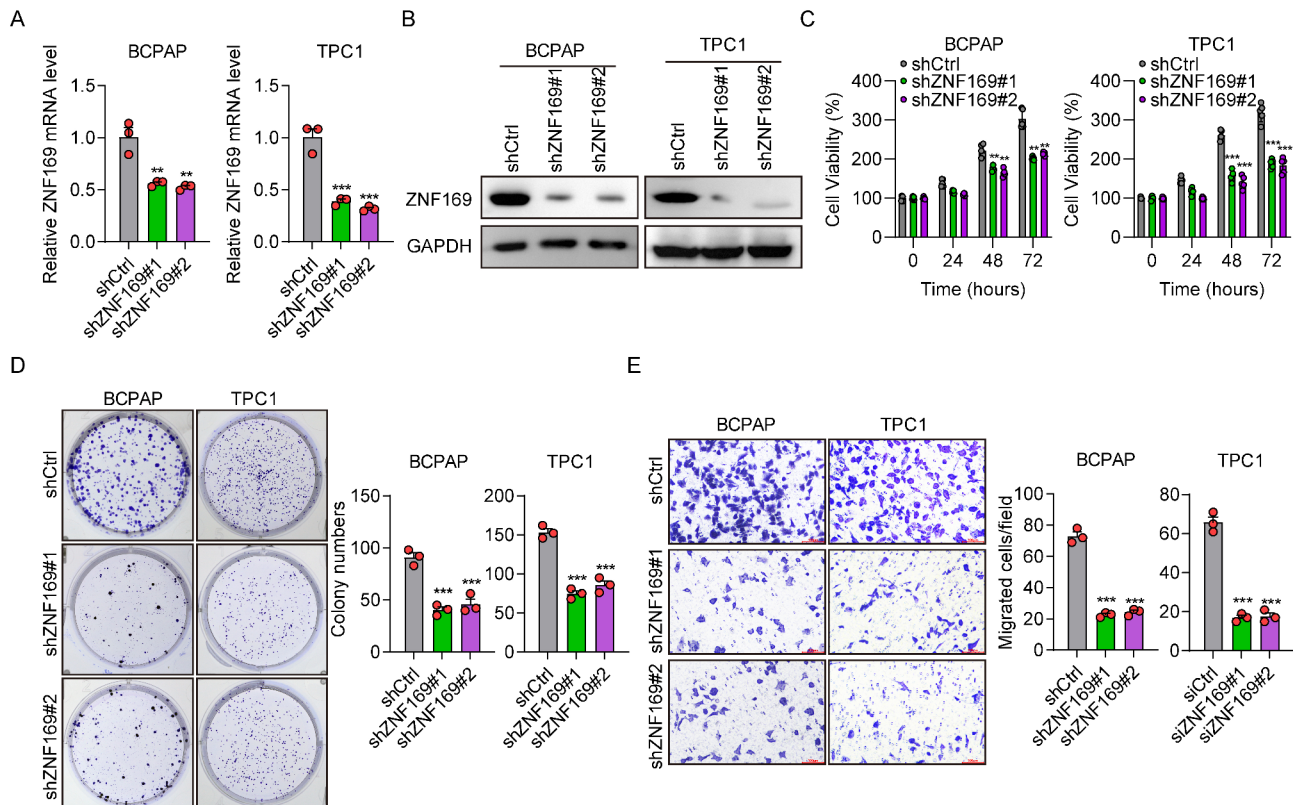


Fig. 2 ZNF169 knockdown suppresses cell proliferation and migration. **(A)** RT-qPCR demonstrated the efficiency of transfection with shCtrl, shZNF169#1 and shZNF169#2 in BCPAP and TPC1 cells. β -actin was used for normalization. **(B)** Western blot analyses demonstrated the efficiency of transfection with shCtrl, shZNF169#1 and shZNF169#2 in BCPAP and TPC1 cells. GAPDH was used as the loading control. **(C)** Cell Counting Kit-8 analysis of BCPAP and TPC1 cells transfected with shCtrl, shZNF169#1 and shZNF169#2. **(D)** Colony formation assay of BCPAP and TPC1 cells transfected with shCtrl, shZNF169#1 and shZNF169#2. **(E)** Transwell invasion analysis of BCPAP and TPC1 cells transfected with shCtrl, shZNF169#1 and shZNF169#2. ** $P < 0.01$, *** $P < 0.001$

was also increased following ZNF169 overexpression compared with those transfected with the control vectors (Fig. 3C). Additionally, ZNF169 overexpression significantly increased the levels of colony formation in K1 cells, with an increase of ~50% compared with control cells (Fig. 3D). Moreover, following ZNF169 overexpression, cell migration was increased 3-fold (Fig. 3E). Consistent with the results of ZNF169 knockdown, ZNF169 overexpression led to downregulation of p21 and E-cadherin, and upregulation of N-cadherin and Vimentin (Figure S1), suggesting that ZNF169 contributes to THCA growth and migration by regulating p21 and EMT signaling.

ZNF169 regulates cell apoptosis and cell cycle progression

Next, we investigated the role of ZNF169 in cell apoptosis and cell cycle progression. ZNF169 knockdown significantly induced cell apoptosis compared with control cells (Fig. 4A). Cell cycle progression analysis also demonstrated that knockdown of ZNF169 decreased the percentage of cells in S stage, while the percentage of cells in G_0/G_1 phases was increased (Fig. 4B). Moreover, apoptosis was inhibited following ZNF169 overexpression

(Fig. 4C). The results of the cell cycle analysis demonstrated that ZNF169 promoted cell cycle progression, with an increased number of S stage cells and a decreased number of G_0/G_1 stage cells (Fig. 4D). Thus, the results of the present study demonstrated that ZNF169 may regulate cell apoptosis and the cell cycle to promote cancer progression.

FBXW10 expression is regulated by ZNF169

To further explore the molecular mechanisms underlying the role of FBXW10, the potential correlation between ZNF169 and FBXW10 was analyzed. A highly positive correlation was revealed between the two genes (Fig. 5A). To determine whether ZNF169 affected the expression of FBXW10, knockdown and overexpression assays were performed. FBXW10 expression was reduced following ZNF169 knockdown and increased following ZNF169 overexpression (Fig. 5B-D). These results were consistent with those obtained using the starBase database (Fig. 5A). To explore whether ZNF169 regulates the transcription activity of FBXW10, we performed luciferase assay. We transfected shZNF169 into TPC1 and BCPAP cells or ZNF169 overexpressing plasmids into K1 cells. ZNF169

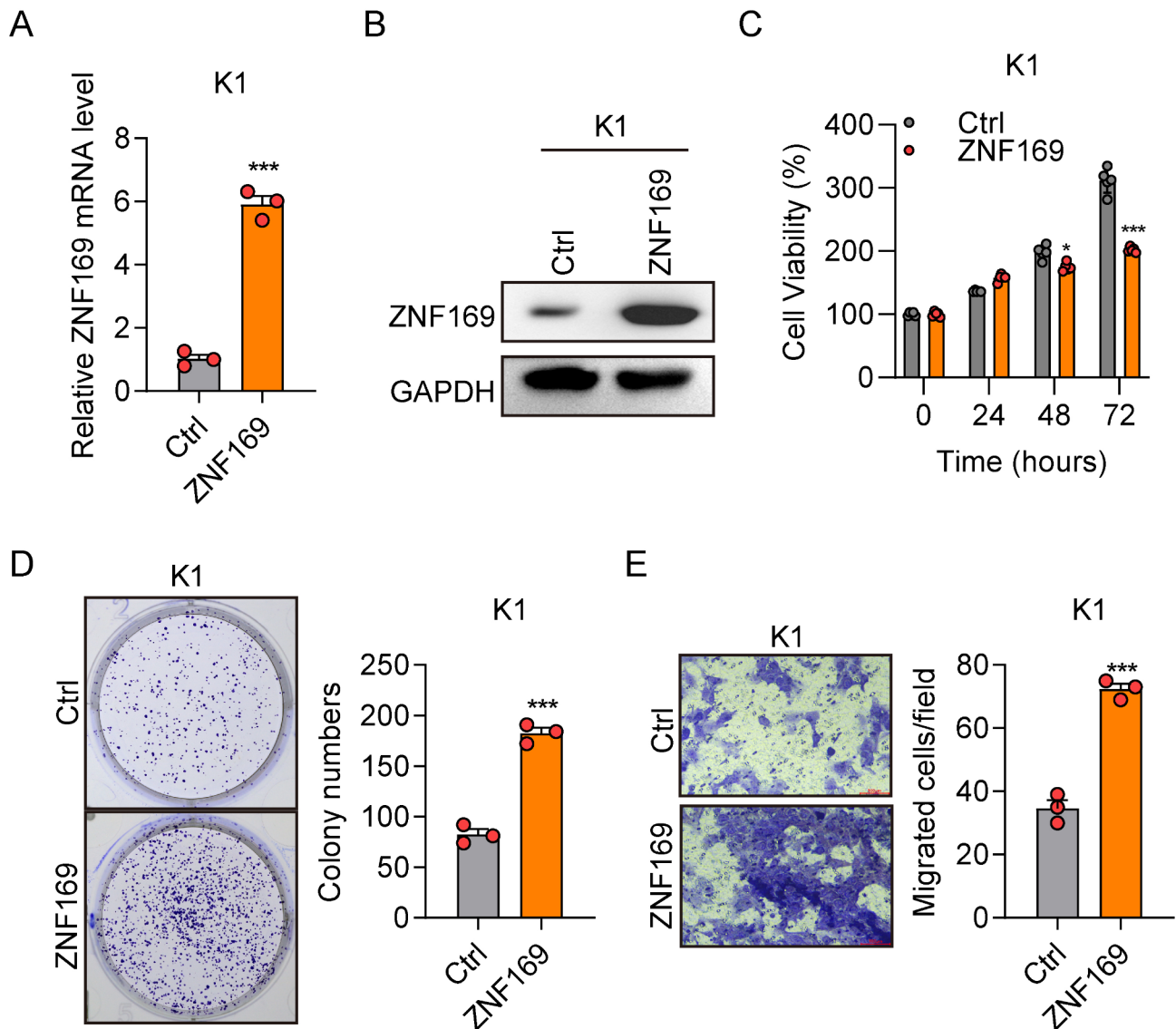
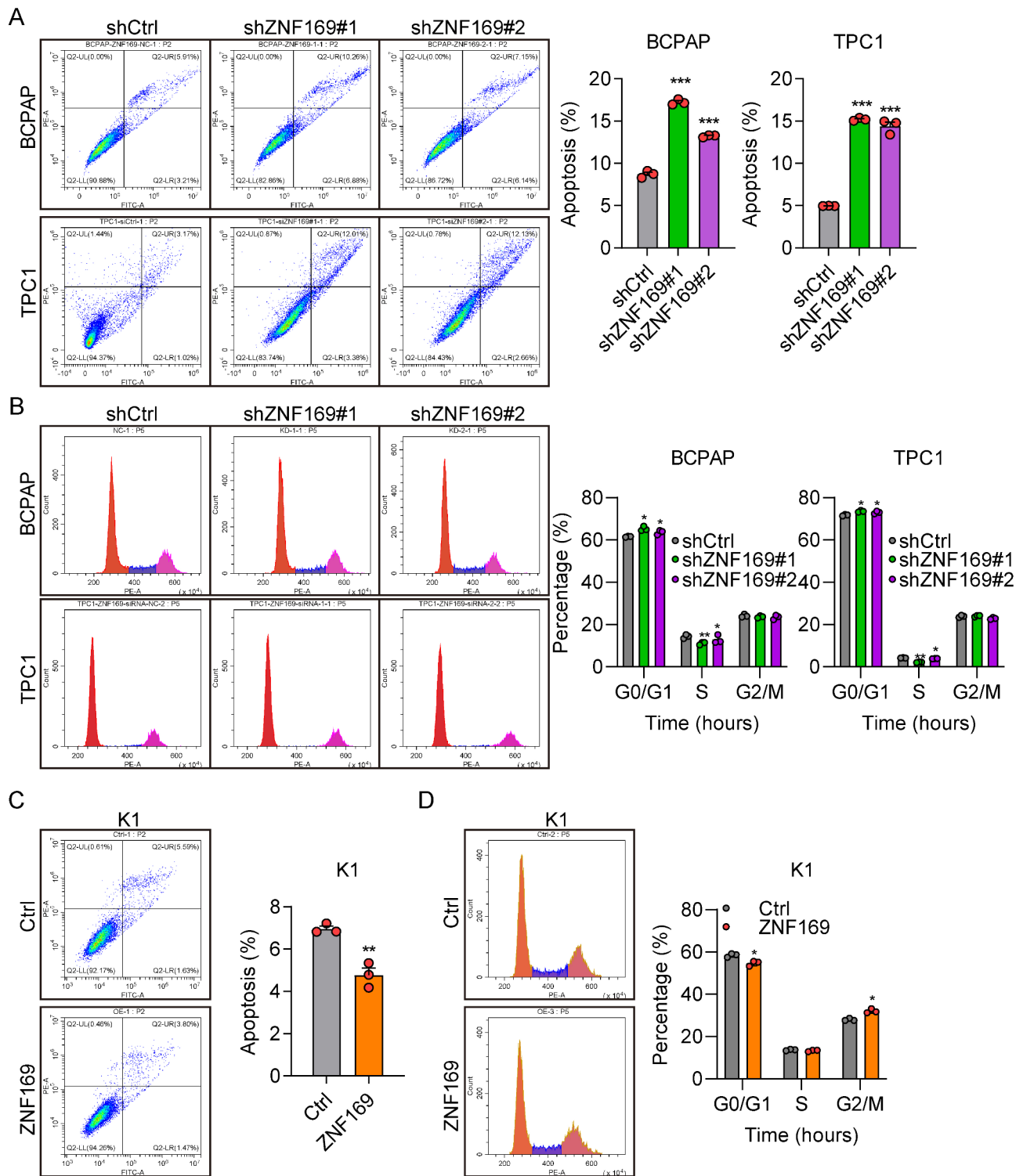


Fig. 3 ZNF169 overexpression promotes cell proliferation and migration. **(A, B)** Overexpression of ZNF169 in K1 cells. RT-qPCR and western blot analyses demonstrated the efficiency of transfection with the ZNF169 overexpression plasmid and Ctrl in K1 cells. β -actin was used for normalization and GAPDH was used as the loading control. **(C)** Cell Counting Kit-8 analysis of K1 cells transfected with the ZNF169 overexpression plasmid and Ctrl. **(D)** Colony formation assay of K1 cells transfected with the ZNF169 overexpression plasmid and Ctrl. **(E)** Transwell invasion analysis of K1 cells transfected with the ZNF169 overexpression plasmid and Ctrl. Magnification: 100 x. ** $P < 0.01$, *** $P < 0.001$

knockdown reduced FBXW10 promoter activity, while ZNF169 overexpression enhanced FBXW10 promoter activity (Fig. 5E). The interaction between ZNF169 and FBXW10 promoter was further confirmed by the ChIP-qPCR and agarose gel electrophoresis assay with the lysates of K1 cells. The results showed that FBXW10 was significantly enriched with the anti-ZNF169 antibody compared to the control IgG (Fig. 5F). Thus, these results demonstrated that ZNF169 regulated the expression of FBXW10 and binding to the promoter of FBXW10.

FBXW10 knockdown inhibits cell proliferation

FBXW10 was previously reported as an oncogene [23, 24]. Thus, the function of FBXW10 was explored in THCA. Western blot and RT-qPCR analyses confirmed the knockdown efficiency following transfection with siFBXW10 in TPC1 cells (Fig. 5G). CCK-8 analyses demonstrated that FBXW10 knockdown markedly reduced the viability of TPC1 cells by ~50% (Fig. 5H). Moreover, a ~50% decrease in the number of colonies was observed following FBXW10 knockdown using a colony formation assay (Fig. 5I). The similar results were obtained in BCPAP cells (Fig. 5J-L). Collectively, these results



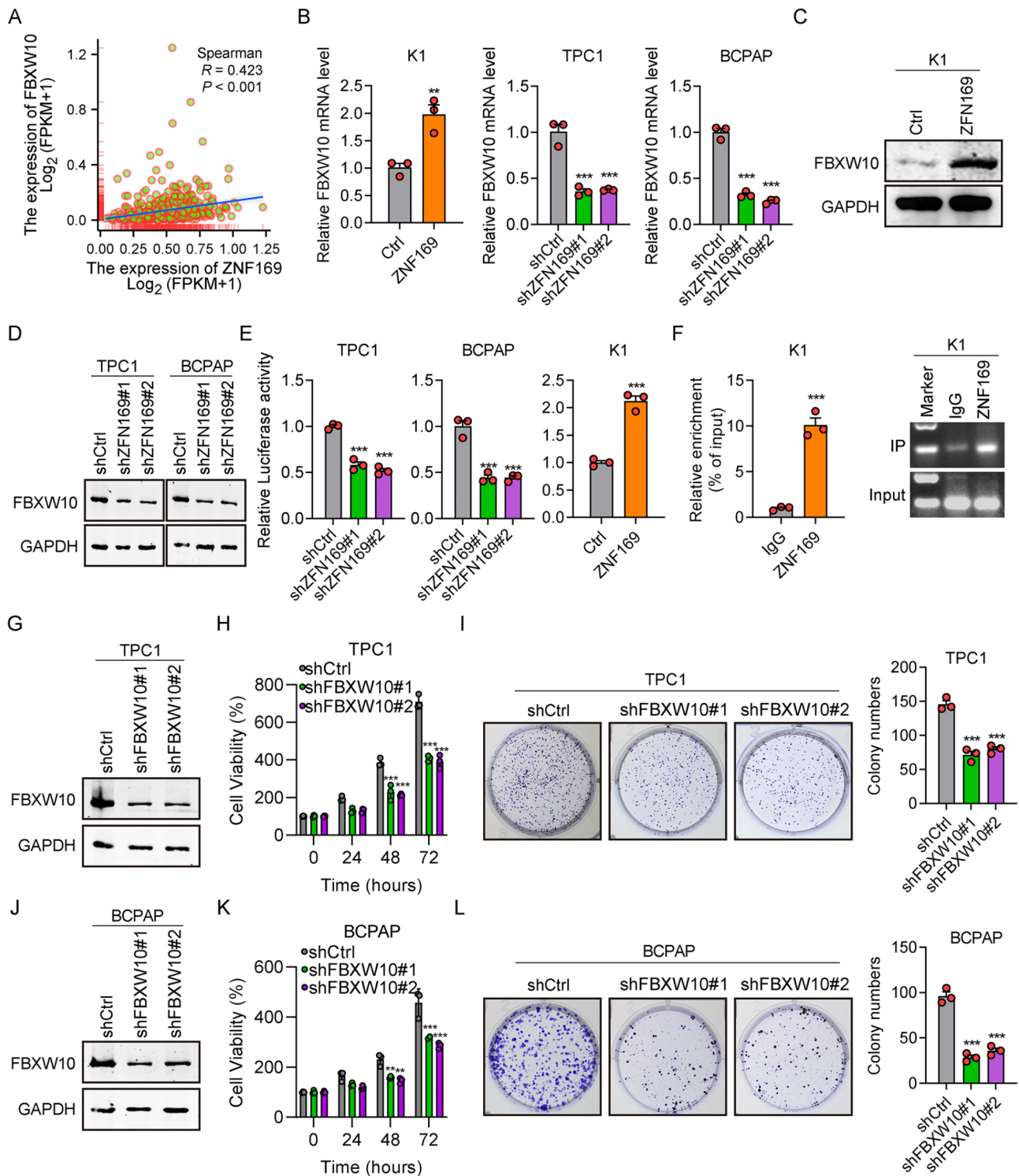


Fig. 5 (See legend on next page.)

demonstrated that FBXW10 may act as an oncogene in THCA.

ZNF169 promotes THCA progression via upregulation of FBXW10

To further elucidate the association between ZNF169 and FBXW10 in THCA, simultaneous overexpression and knockdown assays were performed in TPC1 and

(See figure on previous page.)

Fig. 5 Expression of FBXW10 is regulated by ZNF169, and FBXW10 knockdown inhibits cell proliferation. **(A)** Correlation between ZNF169 and FBXW10 expression ($n = 510$). THCA, thyroid carcinoma. **(B)** RT-qPCR analyses of FBXW10 expression in K1 cells transfected with the ZNF169 overexpression plasmid and Ctrl, and BCPAP and TPC1 cells transfected with shCtrl, shZNF169#1 and shZNF169#2. β -actin was used for normalization. **(C)** Western blot analyses of FBXW10 expression in K1 cells transfected with the ZNF169 overexpression plasmid and Ctrl. **(D)** Western blot analyses of FBXW10 expression in BCPAP and TPC1 cells transfected with shCtrl, shFBXW10#1 and shFBXW10#2. GAPDH was used as the loading control. **(E)** The binding relationship between ZNF169 and the FBXW10 promoter was analyzed by dual-luciferase reporter assay. **(F)** qPCR analysis shows FBXW10 levels that are pulled down in ChIP assay with the anti-ZNF169 antibody or IgG. The qPCR product was subjected to agarose gel electrophoresis. K1 cell lysates were used for the ChIP assay. **(G)** The knockdown efficiency of FBXW10 in TPC1 cells transfected with shCtrl, shFBXW10#1 and shFBXW10#2. **(H)** Cell Counting Kit-8 analysis of TPC1 cells transfected with shCtrl, shFBXW10#1 and shFBXW10#2. **(I)** Colony formation assay of TPC1 cells transfected with shCtrl, shFBXW10#1 and shFBXW10#2. **(J)** The knockdown efficiency of FBXW10 in BCPAP cells transfected with shCtrl, shFBXW10#1 and shFBXW10#2. **(K)** Cell Counting Kit-8 analysis of BCPAP cells transfected with shCtrl, shFBXW10#1 and shFBXW10#2. **(L)** Colony formation assay of BCPAP cells transfected with shCtrl, shFBXW10#1 and shFBXW10#2. * $P < 0.05$, ** $P < 0.01$, *** $P < 0.001$

K1 cells. Western blot results showed that the expression of FBXW10 was reduced by ZNF169 knockdown and was recovered following FBXW10 overexpression in TPC1 cells (Fig. 6A). CCK-8 viability and colony formation assays showed that FBXW10 overexpression recovered the decreased cell viability and cell colony numbers in TPC cells with ZNF169 knockdown (Fig. 6B and C). On the other hand, western blot analysis demonstrated that FBXW10 was upregulated by ZNF169 overexpression and reduced following FBXW10 knockdown in K1 cells (Fig. 6D). Cell viability and colony formation promoted by ZNF169 overexpression could be reversed by FBXW10 knockdown in K1 cells (Fig. 6E and F). Lastly, we performed recovery assay in animal experiments. To validate the effect of ZNF169 and FBXW10 on the tumorigenesis of THCA cells, we applied nude mice which were widely used in the research of cancer cell growth and proliferation in vivo. K1 cells transfected with ZNF169, or ZNF169 + shFBXW10, and the corresponding control (Ctrl) were injected into the flank region of the nude mice. The xenograft tumor size, volume, and weight derived from ZNF169 overexpressing K1 cells were significantly higher compared to the Ctrl ones, while these from the ZNF169 + shFBXW10 group were greatly lower compared to ZNF169 group (Fig. 6G-I). Collectively, ZNF169 contributes to THCA cell proliferation and tumorigenesis through upregulation of FBXW10. The in vivo results may reveal the tumor progression of THCA patients who had overexpression of ZNF169 and FBXW10.

Discussion

The thyroid gland is located in the neck, and is one of the most important endocrine organs in humans, secreting metabolic hormones crucial for the regulation of systemic metabolism [27]. The accumulation of mutant thyroid gland cells leads to the development of THCA. Thyroid cancer is the most common type of endocrine cancer, and early diagnosis leads to more effective treatment options [28, 29]. Thus, further investigations into the mechanisms underlying THCA progression are

required to achieve earlier diagnosis and develop novel treatment options.

The results of the present study demonstrated that both ZNF169 and FBXW10 acted as oncogenes in THCA, as ZNF169 or FBXW10 knockdown led to reduced levels of cell proliferation and invasion. In addition, the expression levels of FBXW10 were reduced following ZNF169 knockdown, and the increased levels of cell proliferation mediated by ZNF169 overexpression were attenuated following FBXW10 knockdown. To the best of our knowledge, the present study is the first to determine the role of the ZNF169/FBXW10 axis in THCA progression, which may lead to the development of more efficient diagnostic strategies and therapeutic options for THCA.

ZNF169 is a nuclear protein that is 603 amino acids in length, which contains one KRAB domain and 13 C2H2-type zinc fingers. A previous study demonstrated that ZNF169 was associated with obesity and ESS1 [22]. Overexpression of ZNF169 has been shown to promote the growth and proliferation of colorectal cancer cells [30]. However, the function of ZNF169 in THCA has yet to be fully elucidated. In the present study, ZNF169 was found to be an oncogene in THCA. ZNF169 was significantly upregulated in THCA tissues. In vitro, we showed that ZNF169 knockdown suppressed the proliferation of THCA cells, while opposite results were observed following ZNF169 overexpression. These results were consistent with the oncogenic function of ZNF169 in colorectal cancer. Besides, we also found that overexpression of ZNF169 potentiated the migration capacity of THCA cells. The results of the present study support those of a previous study that demonstrated the tumor-promoting function of ZNF169 in other malignancy [30]. Although the overall function of ZNF169 was examined in the present study, further investigation is required to determine the specific biological mechanisms underlying the role of ZNF169. Future studies must also focus on determining the specific type of THCA associated with ZNF169, as multiple types have been reported, including PTC, FTC, MTC and ATC [31, 32], and each type of THCA is characterized by a different set of genetic

mutations [12, 32]. Thus, ZNF169 may have the potential to serve as a diagnostic marker for a specific type of THCA.

To further explore the underlying mechanisms of ZNF169 in the development of THCA, we analyzed the expression levels of ZNF169 and FBXW10 using public database and found that there was a positive correlation between ZNF169 and FBXW10. In turn, we next investigated whether ZNF169 plays its important functions through regulating FBXW10. FBXW10 is located on chromosome 17p12 and belongs to the FBXW family of protein ubiquitin ligases [23–26]. The results of a previous study demonstrated that methylation of FBXW10 was increased in clear cell renal cell carcinoma cancer tissues, and this was significant for tumor invasion [23, 33]. Thus, the methylation status of FBXW10 in THCA cells or patient samples requires further investigation. Moreover, the results of the present study demonstrated that ZNF169 knockdown reduced the expression levels of FBXW10. Future investigations should focus on determining whether the reduced expression of FBXW10 is due to increased levels of methylation, as zinc fingers are transcriptional regulation motifs [22]. As previous indicated, FBXW10 was acted as an oncogene to promote hepatocarcinogenesis [24]. Mechanistic evidences showed that FBXW10 promoted HCC development through regulating S6K1-ANXA2-KRAS-ERK axis [34]. In addition, FBXW10 suppression of LATS2 protein stability potentiated the angiogenesis and hepatic metastasis of colorectal cancer [35]. Here, we determined the potential roles of FBXW10 in the development of THCA. Our results suggested that suppression of FBXW10 expression obviously inhibited THCA cell proliferation and colony formation *in vitro*. We also demonstrated that knockdown of FBXW10 completely reversed the accelerated THCA cell growth and tumorigenesis which were promoted by ZNF169. These results suggested that upregulation of FBXW10 was critical for ZNF169-triggered THCA progression. However, further investigations should also focus on determining the specific mechanisms underlying FBXW10 in THCA, and whether there are alternate proteins that participate in the aforementioned processes. Moreover, the potential role of the tumor microenvironment in modulating the effects of ZNF169 and FBXW10 on THCA progression should be conducted on immune-sufficient animal models in the future. Collectively, understanding the molecular events, biological function or immune escape involvement of FBXW10 in THCA in the follow up study will largely help us develop novel drug targets for THCA patients.

Owing to the potential association between ZNF169 and FBXW10, our results of the present study demonstrated that FBXW10 expression was reduced following ZNF169 knockdown. We also showed that ZNF169

enhanced the transcription activity of FBXW10 gene via direct binding to its promoter, whereas ZNF169 binding sequences in the promoter region of FBXW10 remain to be fully elucidated. And we further confirmed that the oncogene roles mediated by ZNF169 in THCA cells could be attenuated by FBXW10 knockdown. Thus, it was hypothesised that FBXW10 may be involved in the ZNF169 pathway and, therefore, may lie downstream of ZNF169. Collectively, the results of the present study revealed that ZNF169 contributes to THCA progression via upregulation of FBXW10. Since ZNF169 is a transcription factor, developing ZNF169 inhibitors for the treatment of THCA may influence the expression of various downstream genes which will cause severe side effects. Thereby, targeting FBXW10 with specific inhibitors maybe a preferable choice for the treatment of THCA patients with overexpression of ZNF169.

Previous studies have reported that transcription co-factors are necessary for the activity of transcription factors in regulating the expression of downstream genes. For instance, pterin-4a-carbinolamine dehydratase 2 (PCBD2) was identified as an essential partner of hepatocyte nuclear factor 1 β (HNF1 β). Cooperation of PCBD2 and HNF1 β plays a pivotal role in regulating genes transcription and the development of the kidney, liver, and pancreas [36]. Signal transducer and activator of transcription 3 (STAT3) is a well-known oncogene in various malignancies [37, 38]. CDK5 kinase regulatory-subunit associated protein 3 (CDK5RAP3) was previously demonstrated as a co-enhancer to potentiate STAT3-dependent gene transcription and the malignancy of cancer cells [39]. Similarly, the regulation of ZNF169 on the transcription of genes, like FBXW10, may also need the cooperation of other co-factors or co-enhancers. We will perform deeper exploration identifying the factors in the follow up study.

In conclusion, to the best of our knowledge, the present study was the first to reveal the oncogenic roles of ZNF169 and FBXW10 in THCA progression, thereby providing a novel theoretical basis for the development of clinical therapies for THCA. Targeting FBXW10 is a promising strategy for the treatment of THCA patients with highly expressed ZNF169.

Materials and methods

Patient samples

A total of 25 patients (18 female and 7 male) with THCA were enrolled in the Hunan Cancer Hospital (Changsha, China) between May 2017 and October 2017. Matched adjacent non-cancerous thyroid tissues of each patient were also used in the present study. The median age of the patients was 44 years (range, 26–66 YEASR). The present study was approved by the Ethics Committee of

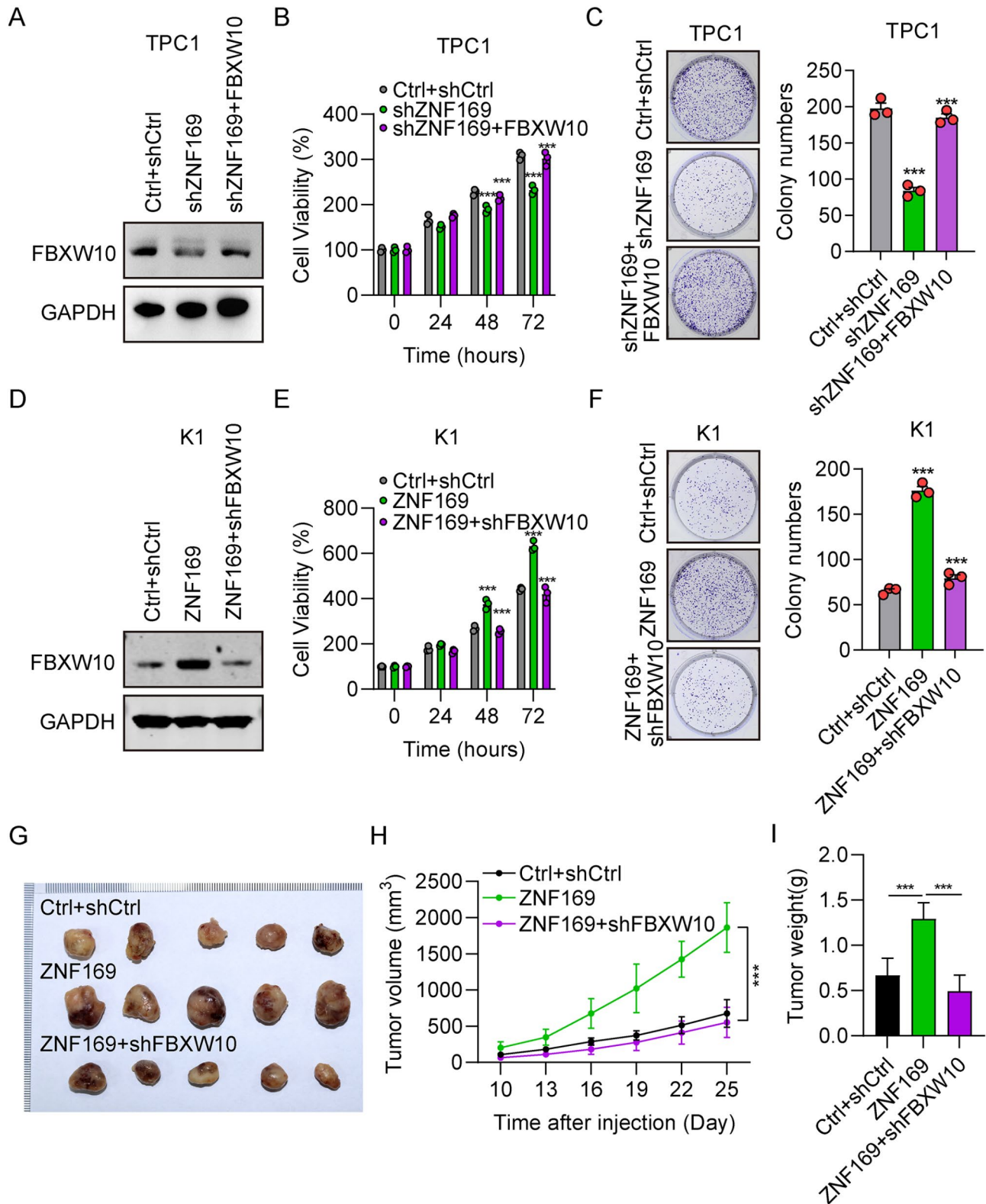


Fig. 6 (See legend on next page.)

(See figure on previous page.)

Fig. 6 Increased cell proliferation mediated by ZNF169 overexpression is attenuated by FBXW10 knockdown. **(A)** Western blot analysis of TPC1 cells transfected with shCtrl+Ctrl, shZNF169 and shZNF169+FBXW10 overexpression plasmid. GAPDH was used as the loading control. **(B)** Cell Counting Kit-8 analysis of TPC1 cells transfected with shCtrl+Ctrl, shZNF169 and shZNF169+FBXW10 overexpression plasmid. **(C)** Colony formation assay of TPC1 cells transfected with shCtrl+Ctrl, shZNF169 and shZNF169+FBXW10 overexpression plasmid. **(D)** Western blot analysis of K1 cells transfected with control, ZNF169 overexpression plasmid and ZNF169 overexpression plasmid+shFBXW10#1. GAPDH was used as the loading control. **(E)** Cell Counting Kit-8 analysis of K1 cells transfected with control, ZNF169 overexpression plasmid and ZNF169 overexpression plasmid+shFBXW10#1. **(F)** Colony formation assay of K1 cells transfected with control, ZNF169 overexpression plasmid and ZNF169 overexpression plasmid+shFBXW10#1. **(G)** Representative images of subcutaneous xenografts in nude mice derived from K1 cells that were treated with control, ZNF169 overexpression plasmid and ZNF169 overexpression plasmid+shFBXW10#1. **(H)** Growth curves of the subcutaneous xenografts in each group. **(I)** Analysis of the tumor weight of the xenografts in each group. ** $P < 0.01$, *** $P < 0.001$

Hunan Cancer Hospital. Written informed consent was obtained from all patients.

Immunohistochemical analysis

ZNF169 staining was carried out using 4- μ m sections from formalin-fixed, paraffin-embedded tissue samples. Briefly, tissue sections were deparaffinized and antigen retrieval was carried out. Following rehydration and blocking with 10% goat serum for 30 min, the slides were incubated with the anti-ZNF169 antibody (1:50; cat. no. ab225924; Abcam) at 4°C overnight. The slides were subsequently washed and incubated with goat anti-rabbit secondary antibody (cat. no. ab6721, Abcam) at room temperature for 1 h, and stained with Vulcan Fast Red Chromogen kit (BIOCARE MEDICAL, Concord, CA, USA) at room temperature for 1 h. The intensity of ZNF169 staining was scored by three independent pathologists as follows: 0, negative; 1, weak staining; 2, moderate staining; and 3, strong staining. A staining score of 0 was defined as negative, and a staining score of 1–3 was defined as positive.

Cell culture and transfection

TPC1 is a thyroid gland papillary carcinoma cell line (0397) purchased from the BCRJ (Rio de Janeiro, Brazil). The website was <http://bcry.org.br/celula/0397>. BCPAP is a poorly differentiated thyroid gland carcinoma cell line (SCSP-543), which were purchased from the Cell Bank of Chinese Academy of Sciences (Shanghai, China). The website was <https://www.cellbank.org.cn/search-detail.php?id=499>. K1 is a thyroid gland carcinoma cell line (GLAG-66), which was purchased from Cellverse (Shanghai, China). The website was <https://www.icellbio.com/cellDetail/5863>. These three cell lines were widely used in the research of THCA. Nthy-ori 3–1 is a normal human primary thyroid follicular epithelial cell (CL-0817) purchased from PROCELL (Wuhan, China). The website was <https://m.procell.com.cn/view/9817>. BCPAP and K1 cells were cultured in DMEM/F-12 medium (Gibco; Thermo Fisher Scientific, Inc.), TPC1 and Nthy-ori 3–1 cells were cultured in RPMI-1640 medium (Procell, Wuhan, China), and supplemented with 2 mM glutamine, 10% FBS (Gibco; Thermo Fisher Scientific, Inc.) and 100 U/ml penicillin/streptomycin

(Sigma-Aldrich; Merck KGaA). The cells were maintained at 37°C under a humidified atmosphere containing 5% CO₂.

Small hairpin (sh)RNAs targeting ZNF169 and FBXW10 were purchased from Shanghai GenePharma Co., Ltd using the pcDNA3.1 vector for stable transfection. The sequences were as follows: shCtrl, 5'-TTCTC CGAACGTGTCACGT-3'; shZNF169#1, 5'-GCCAGA AGTCTCACTTGCATA-3'; and shZNF169#2, 5'-CGC CAGAAGATAGCCCTCCTT-3'; shFBXW10#1: 5'-GT CCTGATAGAGGAGAGAAAT-3'; and shFBXW10#2: 5'-CGGGAGCTATGACCTAAGTAT-3'. Lipofectamine® RNAiMAX transfection reagent (Invitrogen; Thermo Fisher Scientific, Inc.) was used for the transfection of shRNAs, according to the manufacturer's protocol. Stably transduced cell populations were selected with puromycin (2 μ g/mL). The overexpression plasmid ZNF169-OE was constructed using pCDH-CMV vector, purchased from Beijing Tianyi Huiyuan Bioscience & Technology Inc., the empty plasmid of pCDH-CMV was used as a negative control. 5 μ g of each plasmid were transfected into the indicated cells using Lipofectamine® 3000 (Thermo Fisher Scientific, Inc.)

Cell counting Kit-8 (CCK-8) assay

CCK-8 reagent was purchased from Sigma-Aldrich; Merck KGaA. Cells were seeded into 96-well plates at a density of 2,000 cells per well. Cells were maintained for the indicated number of days, followed by the addition of 10 μ l CCK-8 reagent at 37°C for 3 h. The absorbance was measured at 450 nm using a microplate reader. The viability of each group at 24, 48 and 72 h was normalized to that at 0 h. Each experiment was repeated at least three times.

Colony formation

TPC1 and BCPAP cells were seeded into six-well plates at a density of 1,000 cells per well, and the culture medium was replaced every 3 days. Colonies formed following cell culture for 14 days at room temperature. Colonies were washed three times using PBS, and subsequently fixed using 4% paraformaldehyde for 20 min at room temperature. Colonies were then stained using Giemsa staining solution for 20 min at room temperature. A total of

> 50 cells were defined as a colony. Each experiment was repeated at least three times.

RNA extraction and reverse transcription-quantitative (RT-q) PCR

TRIzol[®] (Thermo Fisher Scientific, Inc.) was used for the isolation of total RNA from cells. RNA was reverse transcribed into cDNA using M-MLV-RTase (Promega Corporation) according to the manufacturer's protocol. qPCR analysis was performed using SYBR Master Mixture (Takara Bio, Inc.) on the Agilent MX3000p Real time PCR system. Primers were used as follows: ZNF169 forward, 5'-GCATCATGTGTGCCCTGAATG-3' and reverse, 5'-GGCCTTCTGGCTAAACCGA-3'; FBXW10 forward 5'-CAGCACGCCATAATTCCG-3' and reverse, 5'-CAACTGCACGTTGGATTGATTT-3'; and β -actin forward, 5'-GAGCTGCGTGTGGCTCCC-3' and reverse, 5'-CCAGAGGCGTACAGGGATAGCA-3'. The $\Delta\Delta C_t$ method was performed to calculate the expression [40]. β -actin was used for normalization.

Apoptosis analysis

eBioscience[™] Annexin V-FITC Apoptosis Detection kit (Thermo Fisher Scientific, Inc.) was used for the determination of cell apoptosis. Cell suspensions were incubated with 5 μ l Annexin V-FITC for 10–15 min. Following incubation, cells were washed using 1X binding buffer and subsequently resuspended in 1X binding buffer. Resuspended cells were incubated with propidium iodide (20 μ g/ml), and samples were subjected to flow cytometry analysis. Each experiment was repeated at least three times.

Cell cycle analysis

ExCycl[™] PI/RNase Staining Solution (Thermo Fisher Scientific, Inc.) was used to analyse the cell cycle according to the manufacturer's protocol. Briefly, cells were trypsinized and centrifuged at 13,000 rpm for 5 min. Following washing with ice-cold D-Hanks buffer (pH 7.2–7.4), cells were fixed using ice-cold 75% ethanol for ~ 1 h. Cells were subsequently centrifuged at room temperature and washed again using D-Hanks buffer, followed by incubation with 0.5 ml of ExCycle[™] PI/RNase staining solution for 15–30 min at room temperature. The samples were analyzed using 488-nm excitation, and emissions were collected using a 585/42 nm bandpass filter or equivalent using a Guava easyCyte HT system (MilliporeSigma).

Western blot analysis

Cells were lysed using RIPA buffer containing proteinase inhibitors (Beyotime Biotechnology). Protein concentration was measured using Bradford reagent (Sigma-Aldrich; Merck KGaA). Subsequently, 20 μ g total protein per lane was separated by SDS-PAGE on a 10% gel. The

separated proteins were transferred onto nitrocellulose membranes and subsequently blocked with 5% non-fat milk at room temperature for 1 h. The membranes were incubated with antibodies against ZNF169 (1:1,000; cat. no. ab225924; Abcam), FBXW10 (1:1,000; cat. no. PA5-43814; Thermo Fisher Scientific, Inc.), and GAPDH (1:1,000; cat. no. 60004-1-Ig; ProteinTech Group, Inc.) at 4°C overnight. Following the primary incubation, the membranes were incubated with the secondary antibody (Thermo Fisher Scientific, Inc.) at room temperature for 1 h.

Transwell assay

A total of 3×10^4 cells/well were seeded into the upper chamber of 24-well FluoroBlok[™] Cell Culture Inserts (Corning, Inc.) to detect cell migration. The lower chambers were filled with DMEM/F-12 medium supplemented with 10% FBS, which served as a chemoattractant. 24 h later, cells that had migrated to the opposite side of the filter at room temperature at least were stained with 0.5% crystal violet ≥ 5 fields counted under an inverted fluorescence microscope. Each experiment was repeated at least three times.

Luciferase assay

The Renilla luciferase (Rluc) and firefly luciferase (Luc) sequences were amplified from the psiCheck 2 vector (Promega, USA). Rluc was placed in the upstream position, and Luc was placed in the downstream position. The FBXW10 sequence along with its 3' UTR was amplified and inserted between Rluc and Luc. Then TPC1, BCPAP cells were seeded into 24-well plates (10^5 cells/well) and transfected with shZNF169#1, shZNF169#2 or shCtrl, and K1 cells was transfected with ZNF169 overexpressing plasmid, or Ctrl, together with luciferase reporter vector. The luciferase activity was determined by normalization to Rluc [41]. Then, the relative activity of other groups was adjusted to the activity of shCtrl or Ctrl group.

Chromatin immunoprecipitation (ChIP)-qPCR

ChIP assay was carried out with a Chromatin Immunoprecipitation Kit (#9005s, Cell Signaling) according to the manufacturer's instructions. K1 cells were fixed with 1% formaldehyde, and the cross-linked chromatin was sonicated to generate 200–800 bp DNA fragments for subsequent immunoprecipitation using antibody against ZNF169. Quantitative analysis of ChIP-derived DNA was performed by qPCR reaction. Subsequently, we subjected the qPCR product to agarose gel electrophoresis. The primer sequences were F: 5'-TGTCCTCTCGCACTCAC TTG-3' and R: 5'-CTCAACTGCACACACAG-3'.

Animal experiments

A total of fifteen 4–6-week-old BALB/c nu mice were purchased from Beijing Vital River Laboratory Animal Technology Co., Ltd. (Beijing, China). K1 cells (10^7 cells) with ZNF169 overexpression, ZNF169 overexpression + shFBXW10, and Ctrl were suspended in 200 μ l PBS and subcutaneously injected into the flank region of mice (five mice per group). Tumor volume was calculated as $\frac{1}{2}$ the maximum (L) \times minimum (W)². The mice were sacrificed after 25 days, the tumor sizes were photographed, and tumor weight were measured. All animal experiments were carried out following the Guide for the Care and Use of Laboratory Animals [42] and approved by the Animal Research Ethics Committee of Hunan Cancer Hospital.

Bioinformatics and statistical analyses

The starBase V3.0 (<http://starbase.sysu.edu.cn/>) database was used to analyse the expression levels of ZNF169 and FBXW10. A potential correlation between ZNF169 and FBXW10 was calculated using 510 samples of thyroid carcinoma (THCA). The data were presented as mean \pm standard deviation and analyzed using GraphPad prism 8.0 (GraphPad Software, Inc.). Unpaired students' t-tests were performed to determine differences between two groups, and one-way ANOVA followed by a Tukey's post hoc test was used for comparisons between ≥ 3 groups. $P < 0.05$ was considered to indicate a statistically significant difference.

Supplementary Information

The online version contains supplementary material available at <https://doi.org/10.1186/s13008-024-00139-5>.

Supplementary Material 1. Figure S1. The expression of E-Cad, N-Cad, Vimentin and P21 after ZNF160 knockdown overexpression.

Acknowledgements

We thanked the pathologists for their contribution to IHC scoring.

Author contributions

Ying Fu designed the study. Wen Luo and Qiyu Xiao conducted the experiments and analyzed the data. Ying Fu and Wen Luo wrote and revised the manuscript.

Funding

This project was supported by Scientific research project of Hunan Provincial Health Commission (20201726) and The science and technology innovation Program of Hunan Province (2021SK51106).

Data availability

No datasets were generated or analysed during the current study.

Declarations

Ethics approval

All procedures performed in studies involving human participants were in accordance with the standards upheld by the Ethics Committee of Hunan Cancer Hospital and with those of the 1964 Helsinki Declaration and its later

amendments for ethical research involving human subjects (approval number: SBQLL-2019-161). All animal experiments were approved by the Ethics Committee of Hunan Cancer Hospital for the use of animals and conducted in accordance with the National Institutes of Health Laboratory Animal Care and Use Guidelines. All animal experiments should comply with the ARRIVE guidelines and conducted in accordance with the U.K. Animals (Scientific Procedures) Act, 1986 and associated guidelines, EU Directive 2010/63/EU for animal experiments (approval number: KNZY-202425).

Statement of informed consent

Written informed consent was obtained from patients.

Competing interests

The authors declare no competing interests.

Received: 4 June 2024 / Accepted: 26 November 2024

Published online: 28 January 2025

References

- Chen DW, Lang BHH, McLeod DSA, Newbold K, Haymart MR. Thyroid cancer. *Lancet* (London England). 2023;401(10387):1531–44. [https://doi.org/10.1016/S0140-6736\(23\)00020-X](https://doi.org/10.1016/S0140-6736(23)00020-X)
- Boucai L, Zafereo M, Cabanillas ME. Thyroid Cancer. A Review. *Jama*. 2024;331(5):425–35. <https://doi.org/10.1001/jama.2023.26348>
- Sung H, Ferlay J, Siegel RL, Laversanne M, Soerjomataram I, Jemal A et al. Global Cancer Statistics 2020: GLOBOCAN Estimates of Incidence and Mortality Worldwide for 36 Cancers in 185 Countries. *CA: a cancer journal for clinicians*. 2021;71(3):209–49. <https://doi.org/10.3322/caac.21660>
- Lim H, Devesa SS, Sosa JA, Check D, Kitahara CM. Trends in Thyroid Cancer Incidence and Mortality in the United States, 1974–2013. *JAMA*. 2017;317(13):1338–48. <https://doi.org/10.1001/jama.2017.2719>
- Araque KA, Gubbi S, Klubo-Gwiezdzinska J. Updates on the Management of Thyroid Cancer. Hormone and metabolic research = Hormon- und Stoffwechselforschung = Hormones et métabolisme. 2020;52(8):562–77. <https://doi.org/10.1055/a-1089-7870>
- Laha D, Nilubol N, Boufraquech M. New therapies for advanced thyroid Cancer. *Front Endocrinol*. 2020;11:82. <https://doi.org/10.3389/fendo.2020.00082>
- Nabhan F, Dedhia PH, Ringel MD. Thyroid cancer, recent advances in diagnosis and therapy. *International journal of cancer*. 2021;149(5):984–92. <https://doi.org/10.1002/ijc.33690>
- Cabanillas ME, Ryder M, Jimenez C. Targeted Therapy for Advanced Thyroid Cancer: Kinase Inhibitors and Beyond. *Endocrine reviews*. 2019;40(6):1573–604. <https://doi.org/10.1210/er.2019-00007>
- Agate L, Minaldi E, Basolo A, Angeli V, Jaccheri R, Santini F et al. Nutrition in Advanced Thyroid Cancer Patients. *Nutrients*. 2022;14(6). <https://doi.org/10.3390/nu14061298>
- Tao Y, Li P, Feng C, Cao Y. New insights into Immune cells and immunotherapy for thyroid Cancer. *Immunol Investig*. 2023;52(8):1039–64. <https://doi.org/10.1080/08820139.2023.2268656>
- Basolo F, Macerola E, Poma AM, Torregrossa L. The 5(th) edition of WHO classification of tumors of endocrine organs: changes in the diagnosis of follicular-derived thyroid carcinoma. *Endocrine*. 2023;80(3):470–6. <https://doi.org/10.1007/s12020-023-03336-4>
- Catalano MG, Poli R, Pugliese M, Fortunati N, Boccuzzi G. Emerging molecular therapies of advanced thyroid cancer. *Mol Aspects Med*. 2010;31(2):215–26. <https://doi.org/10.1016/j.mam.2010.02.006>
- Baloch ZW, Asa SL, Barletta JA, Ghossein RA, Juhlin CC, Jung CK, et al. Overview of the 2022 WHO classification of thyroid neoplasms. *Endocr Pathol*. 2022;33(1):27–63. <https://doi.org/10.1007/s12022-022-09707-3>
- Wei X, Wang X, Xiong J, Li C, Liao Y, Zhu Y, et al. Risk and prognostic factors for BRAF(V600E) mutations in papillary thyroid carcinoma. *Biomed Res Int*. 2022;2022(9959649). <https://doi.org/10.1155/2022/9959649>
- Fallahi P, Ferrari SM, Galdiero MR, Varricchi G, Elia G, Ragusa F et al. Molecular targets of tyrosine kinase inhibitors in thyroid cancer. *Seminars in cancer biology*. 2022;79:180–96. <https://doi.org/10.1016/j.semcancer.2020.11.013>
- Odate T, Oishi N, Vuong HG, Mochizuki K, Kondo T. Genetic differences in follicular thyroid carcinoma between Asian and western countries: a systematic review. *Gland Surg*. 2020;9(5):1813–26. <https://doi.org/10.21037/gs-20-356>
- Oh Y, Park JH, Djunadi TA, Shah Z, Chung LI, Chae YK. Deep response to a combination of mTOR inhibitor temsirolimus and dual immunotherapy of

- nivolumab/ipilimumab in poorly differentiated thyroid carcinoma with PTEN mutation: a case report and literature review. *Frontiers in endocrinology*. 2024;15:1304188. <https://doi.org/10.3389/fendo.2024.1304188>.
18. Petrulea P MS, Plantinga TS, Smit JW, Georgescu CE, Netea-Maier RT. PI3K/Akt/mTOR: a promising therapeutic target for non-medullary thyroid carcinoma. *Cancer Treat Rev*. 2015;41(8):707–13. <https://doi.org/10.1016/j.ctrv.2015.06.005>
 19. Heidari Z, Harati-Sadegh M, Arian A, Maruei-Milan R, Salimi S. The effect of TP53 and P21 gene polymorphisms on papillary thyroid carcinoma susceptibility and clinical/pathological features. *IUBMB Life*. 2020;72(5):922–30. <https://doi.org/10.1002/iub.2225>
 20. Cameselle-Teijeiro JM, Peteiro-González D, Caneiro-Gómez J, Sánchez-Ares M, Abdulkader I, Eloy C et al. Cribriform-morular variant of thyroid carcinoma: a neoplasm with distinctive phenotype associated with the activation of the WNT/ β -catenin pathway. *Modern pathology: an official journal of the United States and Canadian Academy of Pathology, Inc*. 2018;31(8):1168–79. <https://doi.org/10.1038/s41379-018-0070-2>.
 21. Turcot V, Lu Y, Highland HM, Schurmann C, Justice AE, Fine RS et al. Protein-altering variants associated with body mass index implicate pathways that control energy intake and expenditure in obesity. *Nat Genet*. 2018;50(1):26–41. <https://doi.org/10.1038/s41588-017-0011-x>.
 22. Levanat S, Chidambaram A, Wicking C, Bray-Ward P, Pressman C, Toftgard R, et al. Pulsed-field gel electrophoresis and FISH mapping of chromosome 9q22: placement of a novel zinc finger gene within the NBCCS and ESS1 region. *Cytogenet Cell Genet*. 1997;76(3–4):208–13. <https://doi.org/10.1159/000134551>
 23. Liu FF, Li HG, Chang H, Wang JL, Lu J. Identification of hepatocellular carcinoma-associated hub genes and pathways by integrated microarray analysis. *Tumori*. 2015;101(2):206–14. <https://doi.org/10.5301/tj.5000241>.
 24. Luo YD, Zhang J, Fang L, Zhu YY, You YM, Zhang CC et al. FBXW10 promotes hepatocarcinogenesis in male patients and mice. *Carcinogenesis*. 2020;41(5):689–98. <https://doi.org/10.1093/carcin/bgz138>.
 25. Aronsson FC, Magnusson P, Andersson B, Karsten SL, Shibasaki Y, Lendon CL, et al. The NIK protein kinase and C17orf1 genes: chromosomal mapping, gene structures and mutational screening in frontotemporal dementia and parkinsonism linked to chromosome 17. *Hum Genet*. 1998;103(3):340–5. <https://doi.org/10.1007/s004390050827>
 26. Jin J, Cardozo T, Lovering RC, Elledge SJ, Pagano M, Harper JW. Systematic analysis and nomenclature of mammalian F-box proteins. *Genes Dev*. 2004;18(21):2573–80. <https://doi.org/10.1101/gad.1255304>.
 27. Cicatiello AG, Di Girolamo D, Dentice M. Metabolic Effects of the Intracellular Regulation of Thyroid Hormone: Old Players, New Concepts. *Front Endocrinol (Lausanne)*. 2018;9:474. <https://doi.org/10.3389/fendo.2018.00474>.
 28. Kondo T, Ezzat S, Asa SL. Pathogenetic mechanisms in thyroid follicular-cell neoplasia. *Nat Rev Cancer*. 2006;6(4):292–306. <https://doi.org/10.1038/nrc1386>.
 29. Paschke R, Lincke T, Muller SP, Kreissl MC, Dralle H, Fassnacht M. The Treatment of Well-Differentiated Thyroid Carcinoma. *Dtsch Arztebl Int*. 2015;112(26):452–8. <https://doi.org/10.3238/arztebl.2015.0452>.
 30. Zhang J, Wang Y, Hou S, Chi X, Ding D, Xue M, et al. Overexpression of ZNF169 promotes the growth and proliferation of colorectal cancer cells via the upregulation of ANKZF1. *Oncol Rep*. 2024;51(6):82. <https://doi.org/10.3892/or.2024.8741>
 31. Sipos JA, Mazzaferri EL. Thyroid cancer epidemiology and prognostic variables. *Clin Oncol (R Coll Radiol)*. 2010;22(6):395–404. <https://doi.org/10.1016/j.clon.2010.05.004>.
 32. Saiselet M, Floor S, Tarabichi M, Dom G, Hebrant A, van Staveren WC et al. Thyroid cancer cell lines: an overview. *Front Endocrinol (Lausanne)*. 2012;3:133. <https://doi.org/10.3389/fendo.2012.00133>.
 33. Wang J, Li J, Gu J, Yu J, Guo S, Zhu Y et al. Abnormal methylation status of FBXW10 and SMPD3, and associations with clinical characteristics in clear cell renal cell carcinoma. *Oncol Lett*. 2015;10(5):3073–80. <https://doi.org/10.3892/ol.2015.3707>.
 34. Liu ZY, Lin XT, Zhang YJ, Gu YP, Yu HQ, Fang L et al. FBXW10-S6K1 promotes ANXA2 polyubiquitination and KRAS activation to drive hepatocellular carcinoma development in males. *Cancer letters*. 2023;566:216257. <https://doi.org/10.1016/j.canlet.2023.216257>.
 35. Zhang ZY, Sun JH, Liang MJ, Wang XP, Guan J, Zhou ZQ. The E3 ubiquitin ligase SCF (FBXW10)-mediated LATS2 degradation regulates angiogenesis and liver metastasis in colorectal cancer. *The international journal of biochemistry & cell biology*. 2023;158:106408. <https://doi.org/10.1016/j.biocel.2023.106408>.
 36. Tholen LE, Bos C, Jansen P, Venselaar H, Vermeulen M, Hoenderop JGJ et al. Bifunctional protein PCBD2 operates as a co-factor for hepatocyte nuclear factor 1 β and modulates gene transcription. *FASEB journal: official publication of the Federation of American Societies for Experimental Biology*. 2021;35(4):e21366. <https://doi.org/10.1096/fj.202002022R>.
 37. Huang B, Lang X, Li X. The role of IL-6/JAK2/STAT3 signaling pathway in cancers. *Frontiers in oncology*. 2022;12:1023177. <https://doi.org/10.3389/fonc.2022.1023177>.
 38. Zou S, Tong Q, Liu B, Huang W, Tian Y, Fu X. Targeting STAT3 in Cancer Immunotherapy. *Molecular cancer*. 2020;19(1):145. <https://doi.org/10.1186/s12943-020-01258-7>.
 39. Egusquiaguirre SP, Liu S, Tošić I, Jiang K, Walker SR, Nicolais M et al. CDK5RAP3 is a co-factor for the oncogenic transcription factor STAT3. *Neoplasia (New York, NY)*. 2020;22(1):47–59. <https://doi.org/10.1016/j.neo.2019.10.002>.
 40. Livak KJ, Schmittgen TD. Analysis of relative gene expression data using real-time quantitative PCR and the 2⁻(Delta Delta C(T)) Method. *Methods*. 2001;25(4):402–8. <https://doi.org/10.1006/meth.2001.1262>.
 41. Li J, Gao X, Zhang Z, Lai Y, Lin X, Lin B et al. CircCD44 plays oncogenic roles in triple-negative breast cancer by modulating the miR-502-5p/KRAS and IGF2BP2/Myc axes. *Mol Cancer*. 2021;20(1):138. <https://doi.org/10.1186/s12943-021-01444-1>.
 42. National Research Council Committee for the Update of the Guide for the Care and Use of Laboratory Animals. *Guide for the Care and Use of Laboratory Animals*. Washington (DC): National Academies Press (US) Copyright © 2011, National Academy of Sciences. 2011.

Publisher's note

Springer Nature remains neutral with regard to jurisdictional claims in published maps and institutional affiliations.